CHEMISTRY
AN ASIAN JOURNAL
www.chemasianj.org

Title: One-pot Synthesis of a Truncated Cone-shaped Porphyrin Macrocycle and Its Self-assembly into Permanent Porous Material

Authors: Ikjin Kim, Avinash Dhamija, In-Chul Hwang, Hochan Lee, Young Ho Ko, and Kimoon Kim

To be cited as: *Chem. Asian J.* 10.1002/asia.202100787

Link to VoR: https://doi.org/10.1002/asia.202100787

A Journal of
ACES
Asian Chemical Editorial Society

A sister journal of **Angewandte Chemie** and **Chemistry – A European Journal**

WILEY-VCH

Chemistry - An Asian Journal 10.1002/asia.202100787

One-pot Synthesis of a Truncated Cone-shaped Porphyrin Macrocycle and Its Self-assembly into Permanent Porous Material

Ikjin Kim†,[a] Avinash Dhamija†,[b] In-Chul Hwang,[b] Hochan Lee,[a] Young Ho Ko,[b] and Kimoon Kim*[b,c]

Dedicated to the memory of Professor Si-Jung Kim (1932 - 2017), one of the founding fathers of the inorganic chemistry division of the Korean Chemical Society.

[a] *I. Kim, H. Lee*
Division of Advanced Materials Science
Pohang University of Science and Technology (POSTECH)
Pohang 37673, Republic of Korea
[b] *Dr. A. Dhamija., Dr. I.-C. Hwang, Dr. Y. H. Ko, Prof. Dr. K. Kim*
Center for Self-assembly and Complexity (CSC)
Institute for Basic Science (IBS)
Pohang 37673, Republic of Korea
Email: kkim@postech.ac.kr
[c] *Prof. Dr. K. Kim*
Department of Chemistry
Pohang University of Science and Technology (POSTECH)
Pohang 37673, Republic of Korea
Email: kkim@postech.ac.kr
[†] *These authors equally contributed in executing the experiments.*

Supporting information for this article is given via a link at the end of the document.

Abstract: Here, we report the synthesis of a truncated cone-shaped triangular porphyrinic macrocycle, $\mathbf{P_3L_3}$, *via* a single step imine condensation of a *cis*-diaminophenylporphyrin and a bent dialdehyde-based linker as building units. X-ray diffraction analysis reveals that the truncated cone-shaped $\mathbf{P_3L_3}$ molecules are stacked on top of each other by $\pi\cdots\pi$ and CH$\cdots\pi$ interactions, to form 1.7 nm wide hollow columns in the solid state. The formation of the triangular macrocycle is corroborated by quantum chemical calculations. The permanent porosity of the $\mathbf{P_3L_3}$ crystals is demonstrated by several gas sorption experiments and powder X-ray diffraction analysis.

Introduction

Macrocycles are one of the most fascinating molecular systems that have played an important role in establishing and developing supramolecular chemistry.[1,2] So far, a wide variety of macrocycles with varying degrees of size, shape, and rigidity have been developed and investigated.[3] One of the important classes of macrocycles includes shape-persistent, truncated cone-shaped skeletons,[4] which are useful for the construction of host molecules, for example, molecular capsules,[5] containers,[6] cavitands,[7] etc.[8] Furthermore, the truncated cone-shaped macrocycles have a tendency to self-assemble into higher-order nanostructures such as channels and columns, which have potential applications in ion transport, sensing, gas separation, construction of liquid crystalline materials.[9] To make better use of the diverse properties of macrocyclic self-assembly, macrocycles must be prepared from easily accessible building blocks by a single-step reaction[10] and have shape-persistency to enhance non-covalent interactions.[11]

In 2020, we reported the synthesis of cuboctahedron shaped gigantic organic cages, the largest one among this kind, *via* the imine condensation of 12 units of tetra(4-aminophenyl)porphyrin and 24 units of 2-hydroxy-1,3-benzendicarboxyaldehyde-based linkers.[12] The X-ray crystal structure of the gigantic porphyrinic cage revealed that the cuboctahedron structure is composed of trimeric and tetrameric porphyrinic macrocycle subunits (Figure S6a). Interestingly, these subunits have unusual truncated cone-like geometries that help in the formation of the gigantic porphyrinic cage. During the investigation on the formation mechanism of the gigantic porphyrinic cage, we envisioned that similar truncated cone-shaped trimeric and tetrameric macrocycles could be synthesized selectively by using a 2-hydroxy-1,3-benzenedicarboxyaldehyde-based linker and a *cis*-di(4-aminophenyl)porphyrin instead of the tetra(4-aminophenyl)porphyrin as building units. Thanks to the truncated cone shape and intrinsic cavity, such macrocycles may self-assemble into porous materials useful for various applications including guest encapsulation and sensing.[8c-e]

Here, we report the construction of a new triangular imine-based porphyrin macrocycle ($\mathbf{P_3L_3}$) *via* an one-pot imine condensation reaction[10,13] of 5,10-bis(4-aminophenyl)-15,20-diphenylporphyrin (**P**) and bent-shaped 5-bromo-2-hydroxy-1,3-benzedicarboxyaldehyde linker (**L**) as building blocks (Figure 1). The resulting shape persistent, truncated cone-shaped $\mathbf{P_3L_3}$ macrocycle maintains an intrinsic cavity, and the solid-state packing of $\mathbf{P_3L_3}$ molecules forms 1D hollow channels, which is confirmed by single crystal X-ray analysis. The permanent porosity of the channels is also demonstrated through several gas sorption and PXRD experiments.

Results and Discussion

Considering the geometries of **P** and **L**, the imine condensation between them would produce, at least in principle, $\mathbf{P_3L_3}$ or $\mathbf{P_4L_4}$ or both (Figure 1). At the outset of this work, therefore, we performed quantum chemical calculations to compare the geometric stability of $\mathbf{P_3L_3}$ and $\mathbf{P_4L_4}$ macrocycles. The optimized structure of $\mathbf{P_3L_3}$ exhibited a truncated cone-shaped geometry, which was also observed in the X-ray crystal structure of the gigantic porphyrinic cage (Figures 1b and S6). The angle between the ditopic linker and the two imine nitrogen atoms (∠NCN', where N and N' denote two imine nitrogen atoms, and C denotes the center of phenyl ring) is 118° (Figure S6b), which is close to that of imine-based architectures using the same linker.[14] On the other hand, the model structure of $\mathbf{P_4L_4}$ showed a distorted planner geometry, in which two ditopic linkers have the ∠NCN' of 112° and the other two have 124°, deviating from the ideal 120° (Figures 1b and S6c). Moreover, the formation energy (ΔE) for $\mathbf{P_3L_3}$ macrocycle in the gas phase is 45.0 kcal/mol lower (more favorable) than that of $\mathbf{P_4L_4}$ macrocycle (Figure S7). These results substantiated that the combination of **P** and **L** would prioritize the formation of $\mathbf{P_3L_3}$ macrocycle over $\mathbf{P_4L_4}$ macrocycle.

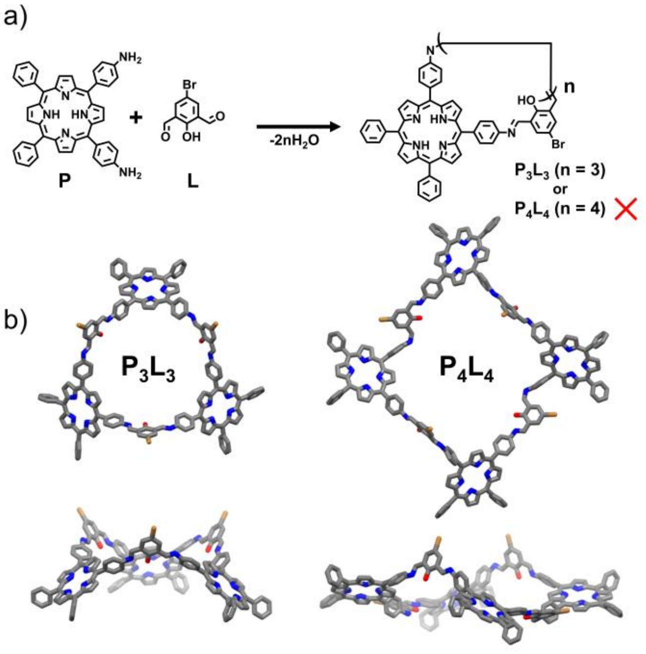

Figure 1. (a) Schematic representation for the design and synthesis of porphyrinic macrocycles. (b) Optimized structures of $\mathbf{P_3L_3}$ and $\mathbf{P_4L_4}$ macrocycles obtained by B3LYP/6-31G(d,p) level of calculations.

As anticipated by the quantum chemical calculations, the reaction of **P** and an equivalent amount of **L** in the presence of a catalytic amount of scandium triflate ($Sc(OTf)_3$) at room temperature for one day resulted in the exclusive formation of the triangular porphyrinic macrocycle, $\mathbf{P_3L_3}$ (Figure 1). MALDI-TOF mass spectrometry revealed a peak at m/z = 2514.9, corresponding to the $[M+H]^+$ ion of $\mathbf{P_3L_3}$ with a molecular formula of $C_{156}H_{100}N_{18}O_3Br_3$ (Figure S1). Mass spectrometry exhibited no trace of $\mathbf{P_4L_4}$ macrocycle. The FTIR spectrum of $\mathbf{P_3L_3}$ clearly showed the emergence of imine C=N stretching bands at 1625 and 1579 cm^{-1} (Figure S2). The ^1H NMR spectrum of $\mathbf{P_3L_3}$ was relatively simple, reflecting the symmetric structure and diffusion-ordered spectroscopy (DOSY) NMR confirmed the existence of a single species ($\mathbf{P_3L_3}$) in solution (Figure S3). In addition, the corresponding hydrodynamic diameter calculated by the Stokes-Einstein equation was around 3.3 nm, which is closer to the expected diameter of $\mathbf{P_3L_3}$ than that of $\mathbf{P_4L_4}$ (Figures S6b and S6c).

In order to grow X-ray diffraction quality single crystals of $\mathbf{P_3L_3}$, slow vapor diffusion of ether (for 1 week) in a 1:1 toluene and carbon disulfide solution of $\mathbf{P_3L_3}$ was carried out, which yielded rectangular-shaped crystals (Figure S8). Single crystal X-ray diffraction (SCXRD) study exhibited that $\mathbf{P_3L_3}$ crystallized in the centrosymmetric triclinic space group, *P*-1, with four $\mathbf{P_3L_3}$ molecules in the unit cell. A close inspection of the crystal structure of $\mathbf{P_3L_3}$ revealed that two conformational isomers of the macrocycle (***A*** and ***B***) exist together depending on the orientation of the imine bonds with respect to the hydroxy group of **L**. In conformer ***A***, three porphyrin units are connected by (*syn-*, *syn-*), (*anti-, anti-*) and (*syn-, anti-*) conformations of the imine bonds. Whereas in conformer ***B***, all porphyrin units are linked by the (*syn-*, *anti-*) conformation of the imine bonds (Figure 2a). The overall shape of the two conformers is best described as a truncated-cone, where three **P** units lean downwards and three **L** units lean upwards, resulting in a cone angle of ~ 120° (Figures S9c and S9d). In the truncated cone-shaped structure of $\mathbf{P_3L_3}$, the minimum diameter (a circle formed by connecting the oxygen atoms of **L**s) and the maximum diameter (a circle formed by connecting the endpoints of **P**s) are estimated to be around 1.7 and 3.2 nm, respectively (Figure S9b), for both ***A*** and ***B*** conformers.

In the crystal, the ***A*** and ***B*** conformers are paired up with the same orientation to form a truncated cone-shaped "supramolecular dimer" ***AB*** *via* CH···*π* and *π*···*π* interactions between slipped porphyrin units and between phenyl groups (Figure S10a). Two neighboring ***AB*** dimers meet at the inversion center, where two ***B*** conformers are interdigitated upside down *via π*···*π* interactions between porphyrin units and phenyl groups (Figure S10b). As a result, the ***A*** and ***B*** conformers form a "supramolecular tetramer" ***ABBA*** (Figure 2c), which acts as a repeating unit to produce 1D hollow columns with a pore diameter of ~ 1.7 nm (Figures S11 and S12). In addition, several short N···H interactions (2.46 ~ 2.70 Å) between the neighboring macrocycles and solvent molecules were observed, which seems to contribute to stabilization of the packing structure of $\mathbf{P_3L_3}$.

To investigate the stability of the crystalline macrocyclic assembly, powder X-ray diffraction (PXRD) studies were performed on the material before and after the removal of solvent molecules. The experimental and simulation PXRD data showed that the crystallinity is well maintained even after removal of solvent molecules by high vacuum treatment (10^{-2} Pa) at 80 °C for 12 h (Figure 3a). Complete desolvation of $\mathbf{P_3L_3}$ crystals after the vacuum treatment and their thermal stability were confirmed by thermogravimetric analysis (TGA) (Figure S5). Furthermore, even after the $\mathbf{P_3L_3}$ crystals were exposed to aqueous media, the diffraction pattern still mostly remained as such, although their shinny faces were lost (Figure S13).

After establishing the presence of 1D channels of $\mathbf{P_3L_3}$ crystals, permanent porosity of $\mathbf{P_3L_3}$ was confirmed by several gas sorption studies. Prior to the gas sorption measurement of $\mathbf{P_3L_3}$ crystals, supercritical CO_2 activation was performed by washing the crystals with liquid CO_2. The N_2 sorption behavior of $\mathbf{P_3L_3}$ crystals followed a type I isotherm with a small hysteresis (Figures 3b and S14). The reason behind the hysteresis is not well understood at the moment, but a similar behavior has been observed in flexible MOFs and organic cages.[15] The Brunauer-Emmett-Teller surface area (S_{BET}) was found to be 205 m^2g^{-1}

(Figure S15a). The pore size distribution obtained by the non-local density functional theory (NLDFT) method showed only a single peak at 1.67 nm (Figure S16), which is close to the pore size of **P_3L_3** observed in the crystal structure (Figure 2c).

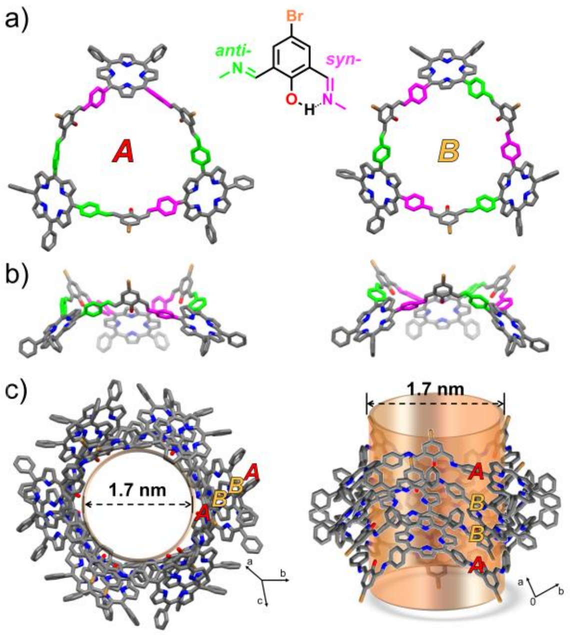

Figure 2. (a) X-ray crystal structure of **P_3L_3** macrocycle depicts two different conformational isomers ***A*** and ***B*** (*anti-* : green, the imine nitrogen is directed away from the hydroxy group; *syn-* : magenta, the imine nitrogen is directed towards the hydroxy group) and (b) their side views. (c) Crystal packing of **P_3L_3** showing a 1.7 nm wide hollow column along [4 1 1] and [0 -2 2] directions (gray: C; blue: N; red: O; orange: Br). Solvent molecules and hydrogen atoms are omitted for clarity.

Next, CO_2 gas sorption experiments were performed for the **P_3L_3** crystals. A CO_2 adsorption isotherm recorded at 195 K revealed a typical type I sorption behavior and produced a S_{BET} value of 360 m^2g^{-1} (CO_2 uptake of 154 cm^3g^{-1} at 1 bar), which is higher than that estimated from the N_2 sorption isotherm (Figures 3c and S15b). Furthermore, gas sorption experiments at 273 K showed that the CO_2 uptake (27.5 cm^3g^{-1} at 1 bar) was superior to N_2 uptake (2.67 cm^3g^{-1} at 1 bar) as well as CO uptake (3.93 cm^3g^{-1} at 1 bar) (Figure 3d). These results may be due to one of the following reasons or both: (i) acidic CO_2 interacts well with relatively basic imine sites in **P_3L_3** packing structure or (ii) CO_2 with a small kinetic diameter (3.3 Å) is readily adsorbed in unexplored narrow sites compared to N_2 (3.64 Å) or CO (3.76 Å).[15c,16] The isosteric heat of adsorption for CO_2 was calculated to be around 36.6 $kJmol^{-1}$ (at 10.6 cm^3g^{-1} uptake of CO_2) by fitting the adsorption data at 195 K and 273 K to the Clausius-Clapeyron equation (Figure S17).

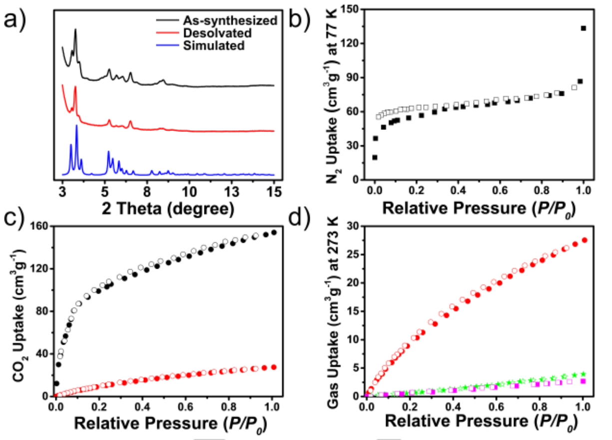

Figure 3. (a) Powder X-ray diffraction profiles of as-synthesized (black), desolvated (red) crystals of **P_3L_3** and simulation data obtained from single crystal structure of **P_3L_3** (blue). (b) N_2 sorption isotherm for **P_3L_3** at 77 K. (c) CO_2 sorption isotherms for **P_3L_3** at 195 K (black) and 273 K (red). (d) CO_2 (red circles), CO (green stars) and N_2 (magenta squares) for **P_3L_3** at 273 K. (solid symbols: adsorption; open symbols: desorption)

Conclusion

We report the facile synthesis of the shape-persistent triangular porphyrinic macrocycle **P_3L_3** *via* imine condensation of 5,10-bis(4-aminophenyl)-15,20-diphenylporphyrin (**P**) and bent-shaped 5-bromo-2-hydroxy-1,3-benzedicarboxyaldehyde linker (**L**) as building blocks. The porphyrinic macrocycle with a truncated cone shape self-assembled into 1D columns in the solid state through $\pi\cdots\pi$ and CH$\cdots\pi$ interactions between porphyrin–porphyrin and porphyrin–phenyl units. This assembly produced a porous architecture containing 1.7 nm wide hollow 1D channels. Permanent porosity of the material was confirmed by several gas sorption experiments and powder X-ray diffraction analysis. Besides the porosity, the macrocyclic assembly can be exploited for various applications by tuning the interior or exterior of the macrocycle through post-synthetic modification of the inner hydroxy group or outer bromine group on the linker. Furthermore, we believe that the approach presented here is applicable to the synthesis of other macrocycles of various sizes by tuning the angle of the bent linker. Work is in progress along these lines.

Acknowledgements

This work was supported by the Institute for Basic Science (IBS) [IBS-R007-D1]. X-ray crystallography experiments with synchrotron radiation were performed at the Pohang Accelerator Laboratory (PLS-II BL2D SMC).

Keywords: Macrocycle • Porous architectures • self-assembly • Imine condensation • permanent porosity

[1] a) J.-M. Lehn, Supramolecular Chemistry: Concepts and Perspectives, Wiley-VCH, Weinheim, **1995**; b) R. M. Izatt, Macrocyclic and Supramolecular Chemistry: How Izatt–Christensen Award Winners Shaped the Field. John Wiley & Sons, Ltd. **2016**; c) F. Diederich, P. J. Stang, R. R. Tykwinski, Modern Supramolecular Chemistry: Strategies for Macrocycle Synthesis. Wiley-VCH Verlag GmbH & Co. KGaA, **2008.**

[2] a) D. J. Cram, *Angew. Chem. Int. Ed. Engl.* **1988**, *27*, 1009–1020; b) J.-M. Lehn, *Angew. Chem. Int. Ed. Engl.* **1988**, *27*, 89–112; c) C. J. Pederson, *Angew. Chem. Int. Ed. Engl.* **1988**, *27,* 1021-1027; d) J. F. Stoddart, *Angew. Chem. Int. Ed.* **2017**, *56*, 11094–11125; e) J.-P. Sauvage, *Angew. Chem. Int. Ed.* **2017**, *56*, 11080–11093.

[3] Reviews on representative macrocycles: a) G. W. Gokel, W. M. Leevy, M. E. Webera, *Chem. Rev.* **2004**, *104*, 2723–2750; b) G. Crini, *Chem. Rev.* **2014**, *114*, 10940–10975; c) C. D. Gutsche, Calixarenes, Royal Society of Chemistry, Cambridge, **1989**; d) K. Kim, Cucurbiturils and Related Macrocycles**,** Royal Society of Chemistry, Cambridge, **2019**; e) T. Ogoshi, T.-A. Yamagishi, and Y. Nakamoto, *Chem. Rev.* **2016**, *116*, 7937–8002; f) Q. He, G. I. Vargas-Zúñiga, S. H. Kim, S. K. Kim, and J. L. Sessler, *Chem. Rev.* **2019**, *119*, 9753-9835; g) f) M. Ball, B. Zhang, Y. Zhong, B. Fowler, S. Xiao, F. Ng, M. Steigerwald, C. Nuckolls, *Acc. Chem. Res.* **2019**, *52*, 1068−1078; h) Y. Nakamura, N. Aratani, A. Osuka, *Chem. Soc. Rev.* **2007**, *36*, 831-845; i) P. S. Bols, H. L. Anderson, *Acc. Chem. Res.* **2018**, *51*, 2083–2092; j) Z. Liu, S. K. M. Nalluri, J. F. Stoddart, *Chem. Soc. Rev.* **2017**, *46*, 2459-2478.

[4] a) W. Zhang, J. S. Moore, *Angew. Chem. Int. Ed.* **2006**, *45*, 4416-4439; b) S. Höger, *Chem. Eur. J.* **2004**, *10*, 1320-1329; c) S. J. Dalgarno, P. K. Thallapally, L. J. Barbour, J. L. Atwood, *Chem. Soc. Rev.* **2007**, *36*, 236-245; d) S. J. Dalgarno, P. K. Thallapally, L. J. Barbour, J. L. Atwood, *Chem. Soc. Rev.* **2007**, *36*, 236-245.

[5] a) V. Ramamurthy, *Acc. Chem. Res.* **2015**, *48*, 2904−2917; b) S. J. Dalgarno, N. P. Power, J. L. Atwood, *Coord. Chem. Rev.* **2008**, *252*, 825–841; c) M. M. Conn, J. Rebek, Jr., *Chem. Rev.* **1997**, *97*, 1647–1668.

[6] a) P. Ballester, M. Fujita, J. Rebek, Jr., *Chem. Soc. Rev.* **2015**, *44*, 392-393; b) S. Zarra, D. M. Wood, D. A. Roberts, J. R. Nitschke, *Chem. Soc. Rev.* **2015**, *44*, 419-432.

[7] a) D. J. Cram, *Science* **1983**, *219*, 1177-1183; b) A. Wishard, B. C. Gibb: A Chronology of Cavitands. (Eds.: Calixarenes and Beyond) Springer, Cham. **2016**; c) F.-U. Rahman, Y.-S. Li, I. D. Petsalakis, G. Theodorakopoulos, J. Rebek, Jr., Y. Yu, *Proc. Natl. Acad. Sci.* **2019**, *116*, 17648-17653.

[8] a) F. Hof, S. L. Craig, C. Nuckolls, J. Rebek, Jr. *Angew. Chem. Int. Ed.* **2002**, *41*, 1488-1508; b) C. J. Brown, F. D. Toste, R. G. Bergman, K. N. Raymond, *Chem. Rev.* **2015**, *115*, 3012–3035; c) J. L. Atwood, L. J. Barbour, A. Jerga, B. L. Schottel, *Science* **2002,** *298*, 1000-1002; d) Y. Zhou, K. Jie, R. Zhao, F, Huang, *Adv. Mater*. **2020**, *32*, 1904824; e) S. Lim, H. Kim, N. Selvapalam, K.-J. Kim, S. J. Cho, G. Seo, K. Kim, *Angew. Chem. Int. Ed.* **2008**, *47*, 3352 –3355; f) H. Kim, Y. Kim, M. Yoon, S. Lim, S. M. Park, G. Seo, K. Kim, J. Am. Chem. Soc. **2010**, *132*, 12200-12202; g) T. Ogoshi, S. Kanai, S. Fujinami, T.-A. Yamagishi, Y. Nakamoto, J. Am. Chem. Soc. **2008**, *130*, 5022-5023; h) K. Jie, M. Liu, Y. Zhou, M. A. Little, S. Bonakala, S. Y. Chong, A. Stephenson, L. Chen, F. Huang, A. I. Cooper, *J. Am. Chem. Soc.* **2017**, *139*, 2908-2911; i) K. Jie, M. Liu, Y. Zhou, M. A. Little, A. Pulido, S. Y. Chong, A. Stephenson, A. R. Hughes, F. Sakakibara, T. Ogoshi, F. Blanc, G. M. Day, F. Huang, A. I. Cooper, *J. Am. Chem. Soc.* **2018**, *140*, 6921-6930.

[9] a) S. Dawn, M. B. Dewal, D. Sobransingh, M. C. Paderes, A. C. Wibowo, M. D. Smith, J. A. Krause, P. J. Pellechia, L. S. Shimizu, *J. Am. Chem. Soc.* **2011**, *133*, 7025–7032; b) L. Mao, Y. Hu, Q. Tu, W.-L. Jiang, X.-L. Zhao, W. Wang, D. Yuan, J. Wen, X. Shi, *Nat. Commun*. **2020**, 5806; c) X. Wu, P. Wang, P. Turner, W. Lewis, O. Catal, D. S. Thomas, P. A. Gale, *Chem* **2019**, *5*, 1210-1222; d) S. H. Kang, Y.-S. Kang, W.-C. Zin, G. Olberechts, K. Wostyn, K, Clays, A. Persoons, K. Kim, *Chem. Commun.* **1999**, 1661-1662; e) A. Chaix, G. Mouchaham, A. Shkurenko, P. Hoang, B. Moosa, P. M. Bhatt, K. Adil, K. N. Salama, M. Eddaoudi, N. M. Khashab, *J. Am. Chem. Soc.* **2018**, *140*, 14571-14575; f) A. Dey, S. Chand, B. Maity, P. M. Bhatt, M. Ghosh, L. Cavallo, M. Eddaoudi, N. M. Khashab, *J. Am. Chem. Soc.* **2021**, *143*, 4090−4094.

[10] a) M. E. Belowich, J. F. Stoddart, Chem. Soc. Rev. **2012**, *41*, 2003-2024; b) K. Acharyya, P. S. Mukherjee, *Angew. Chem. Int. Ed.*, **2019**, *58*, 8640-8653.

[11] a) M. J. Strauss, M. Jia, A. M. Evans, I. Castano, R. L. Li, X. Aguilar-Enriquez, E. K. Roesner, J. L. Swartz, A. D. Chavez, A. E. Enciso, J. F. Stoddart, M. Rolandi, W. R. Dichtel, *J. Am. Chem. Soc.* **2021**, *143*, 8145−8153; b) M. J. Strauss, D. Asheghali, A. M. Evans, R. L. Li, A. D. Chavez, C. Sun, M. L. Becker, W. R. Dichtel, *Angew. Chem. Int. Ed.* **2019**, *58*, 14708-14714; c) S. Wang, A. D. Chavez, S. Thomas, H. Li, N. C. Flanders, C. Sun, M. J. Strauss, L. X. Chen, A. J. Markvoort, J.-L. Bredas, W. R. Dichtel, *Chem. Mater*. **2019**, *31*, 7104-7111.

[12] J. Koo, I. Kim, Y. Kim, D. Cho, I.-C. Hwang, R. D. Mukhopadhyay, H. Song, Y. H. Ko, A. Dhamija, H. Lee, W. Hwang, S. Kim, M.-H. Baik, K. Kim, *Chem* **2020**, *6*, 3374-3384.

[13] a) S. J. Rowan, S. J. Cantrill, G. R. L. Cousins, J. K. M. Sanders, J. F. Stoddart, *Angew. Chem. Int. Ed.* **2002**, *41*, 898−952; b) P. T. Corbett, J. Leclaire, L. Vial, K. R. West, J.-L. Wietor, J. K. M. Sanders, S. Otto, *Chem. Rev.* **2006**, *106*, 3652−3711.

[14] a) S. Brooker, G. S. Dunbar, T. Weyhermuller, *Supramol. Chem.* **2001**, *13*, 601-612; b) J. Gao, J. H. Reibenspies, R. A. Zingaro, F. R. Woolley, A. E. Martell, A. Clearfield, *Inorg. Chem.* **2005**, *44*, 232-241; c) A. Arbaoui, C. Redshaw, D. L. Hughes, *Supramol. Chem*. **2009**, *21*, 35-43; d) K. Tanaka, R. Shimoura, M. R. Caira, *Tetrahedron Lett.* **2010**, *51*, 449-452; e) M. Mastalerz, M. W. Schneider, I. M. Oppel, O. Presly, *Angew. Chem. Int. Ed.* **2011**, *50*, 1046-1051; f) W. Yang, K.-Q. Zhao, T. J. Prior, D. L. Hughes, A. Arbaoui, M. R. J. Elsegood, C. Redshaw, *Dalton Trans.* **2016**, *45*, 11990-12005; g) M. Petryk, A. Janiak, L. J. Barbour, M. Kwit, *Eur. J. Org. Chem.* **2018**, 1916-1923.

[15] a) A. Schneemann, V. Bon, I. Schwedler, I. Senkovska, S. Kaskel, R. A. Fischer, *Chem. Soc. Rev.* **2014**, *43*, 6062-6096; b) T. Mitra, X. Wu, R. Clowes, J. T. A. Jones, K. E. Jelf, D. J. Adams, A. Trewin, J. Bacsa, A. Steiner, A. I. Cooper, *Chem. Eur. J.* **2011**, *17*, 10234-10240; c) S. Hong, M. R. Rohman, J. Jia, Y. Kim, D. Moon, Y. Kim. Y. H. Ko, E. Lee, K. Kim, *Angew. Chem. Int. Ed*. **2015**, *54*, 13241-13244.

[16] a) Z. Zhang, Z.-Z. Yao, S. Xiang, B. Chen, *Energy Environ. Sci*. **2014**, *7*, 2868-2899; b) J. Lü, C. P.-Krap, M. Suyetin, N. H. Alsmail, Y. Yan, S. Yang, W. Lewis, E. Bichoutskaja, C. C. Tang, A. J. Blake, R. Cao, M. Schröder, *J. Am. Chem. Soc*. **2014**, *136*, 12828-12831; c) N. Huang, X. Chen, R. Krishna, D. Jiang, *Angew. Chem. Int. Ed*. **2015**, *54*, 2986-2990; d) R. S. Patil, D. Banerjee, C. Zhang, P. K. Thallapally, J. L. Atwood, *Angew. Chem. Int. Ed*. **2016**, *55*, 4523-4526.

10.1002/asia.202100787

Entry for the Table of Contents

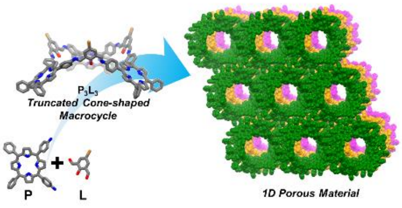

One-pot imine condensation of a *cis*-diaminophenylporphyrin and a bent dialdehyde-based linker as building units produce a shape-persistent truncated cone-shaped macrocycle, which self-assembles into a 1D porous material with 1.7 nm wide hollow channels in the solid state.